A Class of Algorithms for Fast Digital Image Registration

DANIEL I. BARNEA, MEMBER, IEEE, AND HARVEY F. SILVERMAN, MEMBER, IEEE

Abstract—The automatic determination of local similarity between two structured data sets is fundamental to the disciplines of pattern recognition and image processing. A class of algorithms, which may be used to determine similarity in a far more efficient manner than methods currently in use, is introduced in this paper. There may be a saving of computation time of two orders of magnitude or more by adopting this new approach.

The problem of translational image registration, used for an example throughout, is discussed and the problems with the most widely used method-correlation explained. Simple implementations of the new algorithms are introduced to motivate the basic idea of their structure. Real data from ITOS-1 satellites are presented to give meaningful empirical justification for theoretical predictions.

Index Terms—Registration efficiency, sequential similarity detection algorithms, spatial cross correlation, spatial registration of digital images.

I. Introduction

THE AUTOMATIC determination of local similarity between two structured data sets is fundamental to the disciplines of pattern recognition and image processing. A class of algorithms, which may be used to determine similarity in a far more efficient manner than methods currently in use, is introduced in this paper. By adopting this new approach there may be a saving of computation time of two orders of magnitude or more.

The method most widely used for similarity detection is correlation. In fact the similarity detection problem itself is generally called "correlation." In this paper, however, the distinction between the mathematical method, correlation, and the class of similarity detection problems will be maintained; for it will be shown that procedures other than those currently in practice will yield efficient and accurate results.

The class of sequential similarity detection algorithms (SSDAs) introduced here may be applied to the entire spectrum of similarity detection problems. A broad theory relating general properties of these algorithms can be developed. In this paper, however, the utility of SSDAs will be illustrated by their application to a specific problem, translational registration, which is basic to image processing.

In Section II, the translational registration problem will be introduced. Section III will describe the computational efficiency of correlation methods. In Section IV some examples of SSDAs are presented in the order they were chronologically investigated. It is intended that this section impart an intuitive feeling about SSDAs to the reader. Section V generalizes this class of algorithms and presents, in light of this general concept, some ideas for further development of the given examples.

Manuscript received May 13, 1971; revised August 6, 1971.

D. I. Barnea was with the IBM T. J. Watson Research Center, Yorktown Heights, N. Y. 10598. He is now with Eljim, Holon, Israel.

H. F. Silverman is with the IBM T. J. Watson Research Center, Yorktown Heights, N. Y. 10598.

II. The Translational Registration Problem

Registration is inherently basic to any image processing system. When it is desired to detect changes or perform a mapping of two similar images, it is necessary for meaningful results to have the images registered. If the pictures do not differ in magnification and rotation, then the best translational fit will yield the required registration. (The problems arising from magnification and rotation will not be considered here for the sake of brevity. However, the methods are applicable when proper modifications are introduced.)

Let two images, S the *search area* and W the *window* be defined as shown in Fig. 1. S is taken as an $L \times L$ array of digital picture elements which may assume one of K grey levels; i.e.,

$$0 \leq S(i, j) \leq K - 1$$
$$1 \leq i, j \leq L.$$

W is considered to be an $M \times M$, M smaller than L array of digital picture elements having the same grey scale range; i.e.,

$$0 \leq W(l, m) \leq K - 1$$
$$1 \leq l, m \leq M.$$

It will be convenient to introduce a notation for $M \times M$ wholly contained subimages.

$$S_M{}^{i,j}(l, m) \equiv S(i + l - 1, j + m - 1), \quad \begin{cases} 1 \leq l, m \leq M \\ 1 \leq i, j \leq L - M + 1. \end{cases} \tag{1}$$

Each $M \times M$ subimage of S can be uniquely referenced by the specification of its upper left corner's coordinates (i, j). These will be used to define *reference points*. It will be assumed that enough *a priori* information is known about the dislocation between the window and search area so that the parameters L and M may be selected with the virtual guarantee that, at registration, a complete subimage is contained in the search area as shown in Fig. 1.

Translational registration, therefore, is a search over some subset of the allowed range of reference points to find a point (i^*, j^*) which indicates a subimage that is most similar to the given window.

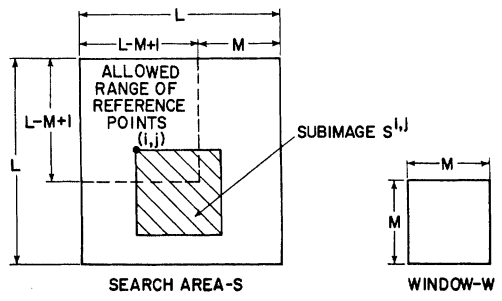

Fig. 1. Search space.

III. Computational Efficiency of Correlation Methods

A. Correlation Method

The method most widely used for the automatic determination of translation is correlation [1], [2]. The elements of the unnormalized cross-correlation surface $R(i, j)$ are defined to be

$$R(i, j) \equiv \sum_{l=1}^{M}\sum_{m=1}^{M} W(l, m)S_M{}^{i,j}(l, m),$$
$$1 \leq i, j \leq L - M + 1. \quad (2)$$

In the correlation scheme a representative output surface such as $R(i, j)$ is searched for a maximum $(\hat{\imath}, \hat{\jmath})$. The procedure is successful if $(\hat{\imath}, \hat{\jmath})$ and (i^*, j^*) are equivalent. As a counterexample, however, consider the unnormalized cross correlation of (2) even in the *ideal case* where W exactly matches some subimage; i.e., $W = S_M{}^{i^*,j^*}$. Then

$$R(i^*, j^*) = \sum_{l=1}^{M}\sum_{m=1}^{M} W^2(l, m). \quad (3)$$

Also, for this ideal case, consider the nonmatching point $(\hat{\imath}, \hat{\jmath})$ where

$$S_M{}^{\hat{\imath},\hat{\jmath}}(l, m) = \max_{l,m} W(l, m) = W_M, \quad \text{for all } (l, m). \quad (4)$$

Clearly

$$R(\hat{\imath}, \hat{\jmath}) = W_M \sum_{l=1}^{M}\sum_{m=1}^{M}, \quad W(l, m) \geq R(i^*, j^*). \quad (5)$$

Therefore even in the ideal case, a search for a maximum over $R(i, j)$ does not necessarily yield the registration point. Normalization is therefore necessary in even the simplest of cases! For completeness, the usual normalized correlation surface is defined in (6).

$$R_N^2(i, j) = \frac{\left(\sum_{l=1}^{M}\sum_{m=1}^{M} W(l, m)S_M{}^{i,j}(l, m)\right)^2}{\left[\sum_{l=1}^{M}\sum_{m=1}^{M} W^2(l, m)\right]\left[\sum_{l=1}^{M}\sum_{m=1}^{M} S_M^2{}^{i,j}(l, m)\right]},$$
$$1 \leq i, j \leq L - M + 1. \quad (6)$$

The choice of a similarity detection algorithm should be justified by its probability for error and its computational complexity rather than by tradition or expediency. Perhaps the two reasons which are generally given for using the correlation method are that: 1) correlation appears to be a natural solution for the mean-square-error criteria [3]; and 2) that analog–optical methods implement correlation easily [4].

However, there is no guarantee for *any* method that a solution is correct or unique. There seems to be, therefore, no adequate justification for the use of correlation to solve all digital registration problems. Algorithms, such as those presented in this paper, which have selectable distance measure properties and lower computational complexity, appear to be a more fitting choice.

B. The Cost of Correlation

The normalized correlation surface may be calculated by direct means or by fast Fourier transform (FFT) methods [5]. In each case the amount of computation required for normalization is the same. The numerator of (6) is all that may be treated by FFT.

In Table I the approximate number of calculations for each procedure are shown. One should note that although the FFT method requires fewer operations for L and M large, this method also requires a memory capacity of $2L^2$ real words which may be infeasible for an L larger than 256.

IV. Some Examples of SSDA Implementation

A. The Basic Concept

For a particular reference point (i, j), there are M^2 points of the subimage $S_M{}^{i,j}$ which may be compared with the M^2 corresponding points in W. (Each set of points for comparison (e.g., $\langle S_M{}^{i,j}(l, m), W(l, m)\rangle$) will be called a *windowing pair.*) In correlation the maximum number of windowing pairs or $M^2(L-M+1)^2$ are compared. Each reference point, regardless of content, is therefore processed with very high precision. However, accuracy is required only for those relatively few points near surface maxima. Hence, there is considerable waste in performing high-accuracy calculations at a vast majority of points.

SSDA reduces this redundancy by performing a sequential search which may be terminated before all M^2 windowing pairs for a particular reference point are tested. Furthermore, the algorithms do not implicitly contain any fixed error measure or measure evaluation method.

B. Constant Threshold Algorithm

A simple but important SSDA has been extensively studied and will be used as a vehicle to introduce the concept. Here, a search over each of the $(L-M+1)^2$ reference points is performed, as in correlation. However, the criteria for similarity at each reference point is significantly different from correlation.

In the constant threshold algorithm, windowing pairs are selected for comparison in a random order so that, in general, a great deal of new information is considered in each test; i.e., a random nonrepeating sequence of the integers $1, 2, \cdots, M^2$ is generated and used to yield the random, nonrepeating sequence of coordinates (l_n, m_n),

TABLE I

COST OF NORMALIZED CORRELATION

Direct Correlation	FFT Correlation	Ordinary Normalization	"Fast" Normalization
$M^2(L-M+1)$-Mults.	$6L^2(\log_2 L)$-Complex Mult-Adds	L^2+M^2-Mults.	L^2+M^2-Mults.
$M^2(L-M+1)^2$-Adds		$M^2(L-M+1)^2$-Adds	$4(L-M+1)^2$-Adds
$(L-M+1)^2$-Squarings	FFT of S,W and IFFT of Product	$(L-M+1)^2$-Mults & Divides	$(L-M+1)^2$-Mults & Divides
	L^2-Complex Mults.		
	$(L-M+1)^2$-Squarings		

$n=1, 2, \cdots, M^2$. Thus the windowing pairs $\langle S_M{}^{i,j}(l_n, m_n), W(l_n, m_n)\rangle$ are compared in random order as n increases.

Unnormalized or normalized measures for evaluating the error between windowing pairs may be defined, respectively, as

$$\epsilon'(i, j, l_n, m_n) \equiv \left| S_M{}^{i,j}(l_n, m_n) - W(l_n, m_n) \right| \quad (7)$$

$$\epsilon(i, j, l_n, m_n) \equiv \left| S_M{}^{i,j}(l_n, m_n) - \hat{S}(i, j) - W(l_n, m_n) + \hat{W} \right| \quad (8)$$

where

$$\hat{W} \equiv \frac{1}{M^2} \sum_{l=1}^{M} \sum_{m=1}^{M} W(l, m) \quad (9)$$

and

$$\hat{S}(i, j) \equiv \frac{1}{M^2} \sum_{l=1}^{M} \sum_{m=1}^{M} S_M{}^{i,j}(l, m). \quad (10)$$

Unlike the correlation methods cited previously, in the *ideal case*, where $W = S_M{}^{i^*,j^*}$, a minimum of zero is guaranteed for the nonnormalized case, i.e., for

$$\|E(i, j)\| \equiv \sum_{l=1}^{M} \sum_{m=1}^{M} \left| S_M{}^{i,j}(l, m) - W(l, m) \right| \quad (11)$$

$$0 = \|E(i^*, j^*)\| \leq \|E(i, j)\|. \quad (12)$$

Thus, in this ideal case no normalization is necessary and, obviously, a comparison of very few points will yield the answer. The error measure, based upon the L_1 norm between two images, is also computationally simpler than the multiplicative measure of correlation.

In this SSDA implementation, a constant threshold T is introduced. As the error for randomly selected windowing pairs is accumulated, a test is made against T. When the accumulated error exceeds T at test N, operations cease for reference point (i, j) and the value N is recorded. The SSDA surface $I(i, j)$ is therefore defined as

$$I(i, j) = \left\{ r \,\middle|\, \min_{1 \leq r \leq M^2} \left\{ \sum_{n=1}^{r} \epsilon(i, j, l_n, m_n) \geq T \right\} \right\}. \quad (13)$$

Reference points where $I(i, j)$ is large (those which require many windowing pair tests to exceed T) are considered points of similarity.

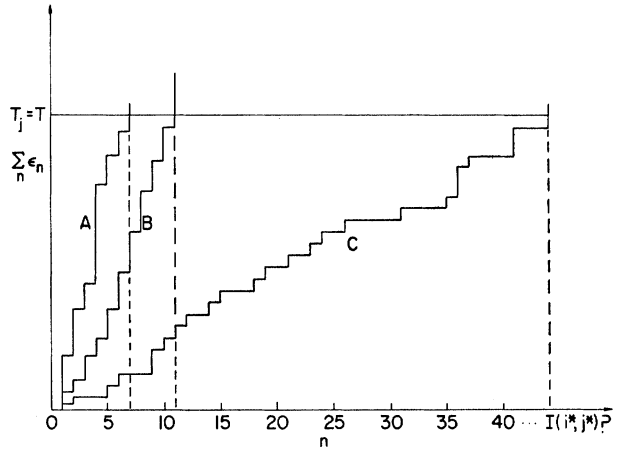

Fig. 2. Growth curves with T=const.

It is clear that if a suitable value for T is selected, many fewer than M^2 tests will be required for reference points which rapidly accumulate error. It is this property which significantly reduces the computational complexity of an SSDA! This fact is made clear by Fig. 2. Curves A, B, and C depict the cumulative error for three different reference points as a function of test. A and B accumulate error rapidly and operations for their reference points terminate early with $I(i, j)$ obtaining values of 7 and 11, respectively. Curve C, however, accumulates error more slowly. It is, therefore, much more likely to be a candidate for registration, and will accordingly have a value of 44 assigned to $I(i, j)$.

Data from the NOAA weather satellite ITOS-1 have been used to test this algorithm. Fig. 3 is an example of a typical data set. Images (a) and (b) are segments of uncorrected vidicon output taken over Baja California on August 9, and 11, 1970, respectively. In this application, one is interested in registering land masses. Therefore, in addition to the noise due to optics and scanners, there is a great deal of intense noise due to clouds and cloud shadow, as well as from the fiducial mark (the $\times$) in (b). Fig. 3(c) shows the window function W taken from the upper left corner of (b). In Fig. 3(d), the answer is displayed. The window of Fig. 3(c) is put into the search area [Fig. 3(a)] at the position indicated by the algorithm.

The fit is visually accurate, but as real rather than contrived data were tested, there is virtually no way to absolutely check this fit. However, the same data were run in an FFT

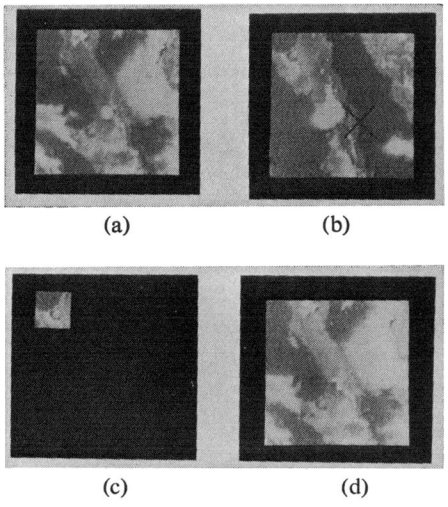

Fig. 3. Example of registered images taken from NOAA data. (a) Search area. (b) Picture 2. (c) Window area taken from (b). (d) Window inserted into search area at (i^*, j^*).

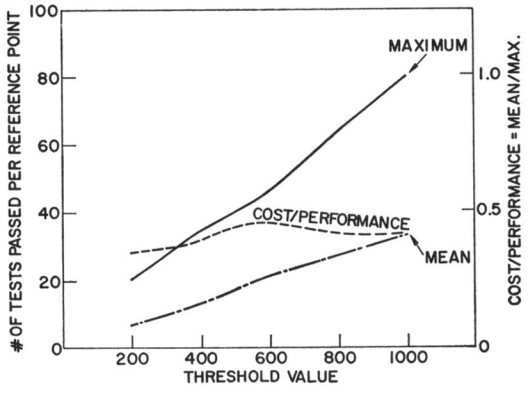

Fig. 4. Statistical results for constant threshold algorithm.

correlation-registration scheme, for the purposes of a relative comparison. As expected, there were some complications involved in the application of this more traditional method. Only after clouds had been detected and their bright surface values replaced by random noise would correlation yield a meaningful peak. (No corrections whatsoever were necessary for SSDA!) For this data, correlation gave the registration point as one picture element higher than did this SSDA. As correct registration might easily lie between two points, there is little to argue!

The data in Fig. 3 have the following attributes:

1) $L=128$;
2) $M=32$;
3) $0 \leq S(i, j) \leq 255$;
4) $E[S(i, j)] \approx 75$ (expected value).

For this data set, tests were made for various values of T. The important results from these tests are given in Fig. 4. The average value of a point in the surface $I(i, j)$—and hence the number of calculations required—grows linearly with threshold. The maximum value in the surface $I(i, j)$, an indicator of the accuracy of the method, also grows linearly with threshold value, although at a somewhat higher rate. The ratio of these two items can be considered as a cost/performance measure. For the case of a constant threshold, this measure is shown to be relatively constant. This implies that accuracy may be achieved only by an associated increase in computation.

C. Monotonic-Increasing Threshold Sequence Algorithm—(Algorithm A)

The growth curve for a particular reference point (three of which are shown in Fig. 2), is a monotonically increasing function. It is the *average slope of the growth curve* that is important in the determination of a threshold crossing. It therefore seems reasonable that the replacement of the constant threshold T by a threshold T_j, increasing monotonically with test, would improve performance when the following criteria are considered.

1) The sequence T_j should have "shape" approximating that of the growth curve for $I(i^*, j^*)$, but should bound this growth curve from above for an arbitrarily large n.

2) The T_j sequence should have initial values high enough so that a trend might be established even for reference points far from registration.

An example of a monotonically increasing threshold sequence is shown in Fig. 5. Growth curves A and B, for reference points far from registration, are eliminated earlier than in Fig. 2, at 4 and 7, respectively. As most reference points do exhibit rapid growth, the total number of tests will be diminished significantly. Growth curve C, however, which appears to be a strong candidate for registration, will undergo a larger number of tests than before. Therefore, a high degree of accuracy will be achieved for those few points which have growth curves with low average slope.

Monotonically increasing threshold curves were generated by several methods. A stochastic approach yielded excellent analytic and experimental results. The distances at registration $\epsilon(i^*, j^*, l, m)$ may be considered a random variable with an exponential distribution

$$f_\alpha(x) = \begin{cases} \dfrac{1}{\lambda} e^{-x/\lambda}, & 0 \leq x \leq \infty \\ 0, & \text{otherwise.} \end{cases} \tag{14}$$

At the point of registration, the sum of "ϵ terms" is a cumulative measure of the noise between two different pictures. At any other reference point $\epsilon(i, j, l, m)$ must be considered as the sum of the noise due to the fact that the pictures are different, *image noise*, and that the pictures are out of registration, *registration noise*. One assumes, in order to say a correct answer has been achieved, that the total noise is minimal at the point of registration.

Optimally, one desires to find a threshold sequence which does the following.

1) It minimizes the probability that a point other than the registration point will remain beneath the threshold as long as the "true" registration point.

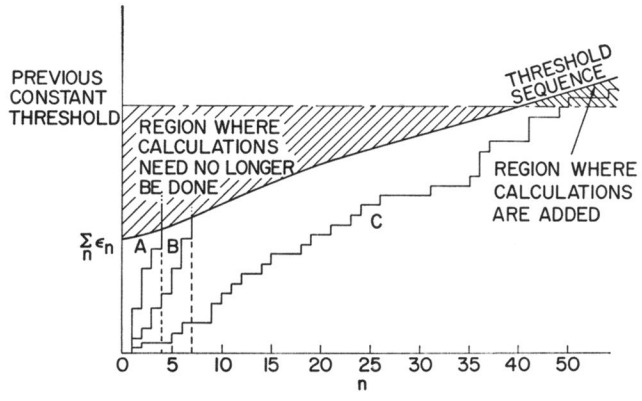

Fig. 5. Growth curve for algorithm Q with T_j a monotonically increasing function.

2) It maximizes the probability that the registration point remains below threshold.

3) It allows the total number of operations to be small.

Some analytic difficulty developed when this total optimization problem was considered. However, suboptimal threshold sequences may be found based upon the image noise alone which appear to satisfy the two hypotheses at the beginning of this section. Empirical results also tend to justify their contention for near optimality.

Fig. 6 shows a set of curves derived simply from the mean and variance of the image noise's statistics. If one has a measure of the mean of this noise λ and a bound to the deviation from the mean that he is willing to allow, he may select a threshold sequence. This method of design, however, leads to results which are somewhat less satisfying than those obtained by more careful derivation.

The curves shown in Fig. 7 are drawn from a computer solution of an analytic system of recursive equations. Here, one considers the probability P_k, which is the probability for the cumulative error at the registration point $I(i^*, j^*)$ to exceed T_k at test k, given that the cumulative error has stayed beneath the threshold for all tests $n=1, 2, \cdots, k-1$. The useful set of design curves of Fig. 7 may be derived by restricting P_k to be a constant q for all k.

While the curves in Figs. 6 and 7 appear to have the same shape, the equiprobable curves, which take into account the results from past as well as present tests, are closer to the optimal. Any particular one of these curves may be generated by an exact set of equations or by an approximate model. Once an estimate to the mean of the image noise λ has been obtained, a reasonable design follows.

Several tests were conducted on the data set shown in Fig. 8. Fig. 8(a) and (b) are each taken from the edge of a large, unnormalized NOAA vidicon output. As before the images were taken two days apart each of the Gulf coast of Texas. The data have many distortions due to sun angle, spacecraft attitude, and optical edge effects. There are also very few prominent features in evidence. The insertion in Fig. 8(d) appears to be correct upon visual inspection.

For this set of data, *a priori* knowledge of the approximate registration point allowed one to find the parameter λ

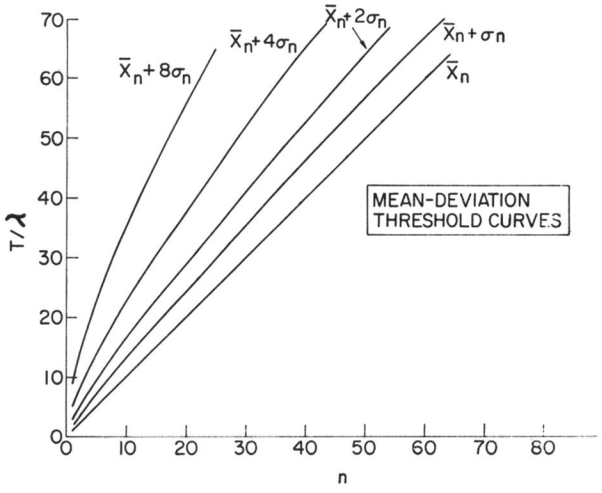

Fig. 6. Mean deviation threshold curves.

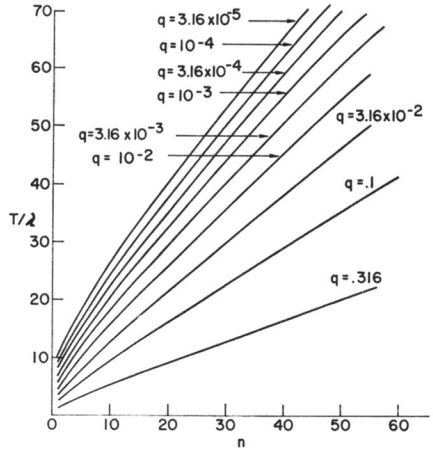

Fig. 7. Calculated equiprobable threshold curves.

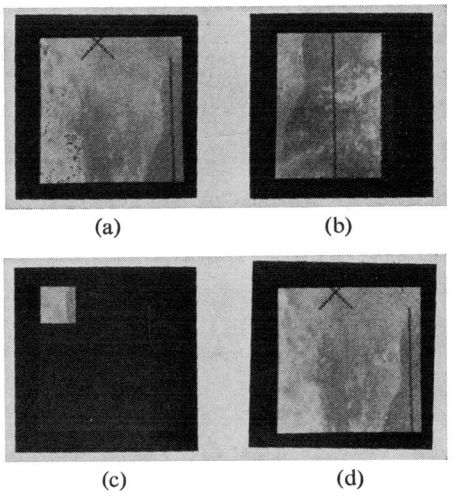

Fig. 8. Second example of registered images taken from NOAA data. (a) Search area. (b) Picture 2. (c) Window area taken from (b). (d) Window inserted into search area at (i^*, j^*).

empirically. Fig. 9 shows the sample distribution for the data of Fig. 8 for the absolute value of the image noise. The exponential distribution assumed in (14) appears to have some justification, with a value of 9.089 for λ. Based upon this data, quantized versions of threshold functions for several values of q were constructed. These are shown in Fig. 10. A quantized approximation was used so that thresholds might be stored in a lookup table and the speed of calculation increased. It was found that a coarse quantization yielded accurate results.

Curves based upon the results of tests on the data of Fig. 8, using the constant q design criteria, are given in Fig. 11. One immediately can see the benefit of using the monotone-increasing threshold sequence by looking at the cost/performance ratio. As one would expect, there is a region where this ratio has minimal—implying optimal—value(s). In the tests conducted, the optimal value(s) for q lie in the range $10^{-2} \leq q \leq 10^{-3}$. Hence, knowledge of the parameter λ and an optimal value for q can lead to a highly efficient design.

D. Computational Aspects

The efficiency of SSDA has been demonstrated in the given examples. The saving which results can be illustrated by relating numbers of operations required for various implementations. Time ratios relating arithmetic operations for the IBM 360/65 will be used. Namely,

1) real multiply time/read add time = 3;
2) real add time/integer add time = 2;
3) integer multiply time/integer add time = 3.5;
4) compare time = integer add time;
5) complex add = 2 real adds;
6) complex multiply = 3 real multiplies + 5 real adds.

From Table I the direct cross-correlation method, *not including normalization*, reduces to

$$\text{number (direct)} = 4.5M^2(L - M + 1)^2 \text{ equivalent integer adds} \quad (15)$$

and the FFT cross-correlation method, *not including normalization*, reduces to

$$\text{number (FFT)} = 200L^2 \log_2 L \text{ equivalent integer adds.} \quad (16)$$

The monotone increasing threshold SSDA, *using the normalized distance measure*, requires:

1) 4 adds/reference point to obtain normalization;
2) 2 adds + 1 compare/windowing point to get the error measure;
3) 1 compare/windowing point;
4) An average of $\bar{n}$ windowing tests/reference point.

Thus

$$\text{number (SSDA)} = (4 + 4\bar{n})(L - M + 1)^2 \text{ equivalent integer adds.} \quad (17)$$

For M of 32, $\bar{n}$ should be about 10–15. However, as M in-

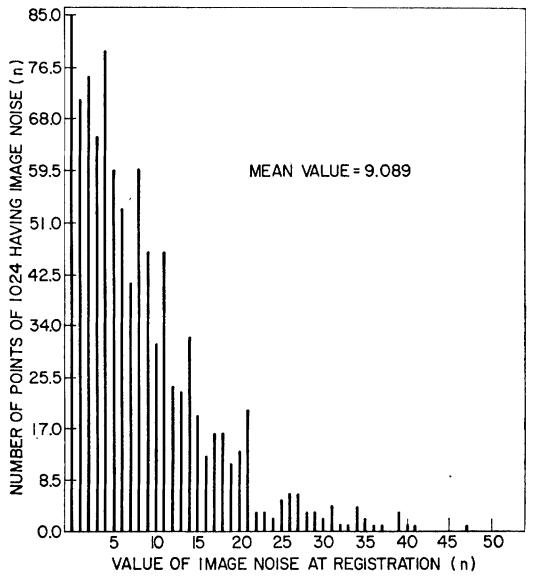

Fig. 9. Sample distribution for image noise for data.

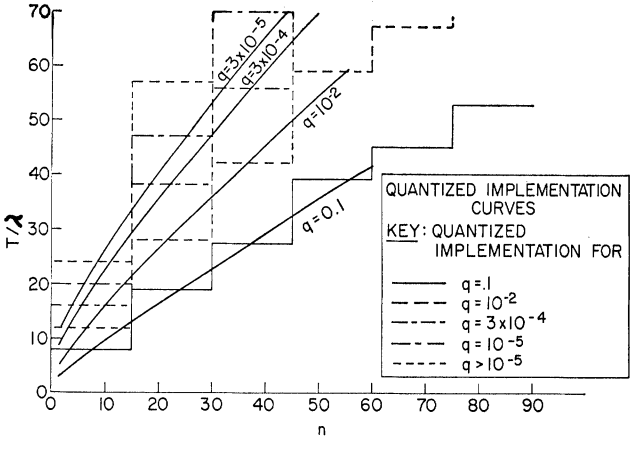

Fig. 10. Quantized implementation of equiprobable curves, where q is the probability for the growth curve at (i^*, j^*) to exceed T_k at any k given that the growth curve is below $T_{k'}$ for all $k' = 1, 2, \cdots, k-1$.

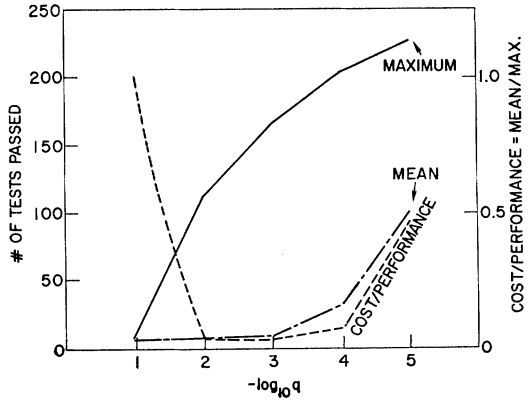

Fig. 11. Statistical results for constant q algorithm.

creases, more points should be checked to establish conclusively that misregistration has occurred. A figure of $\bar{n} = 10(M/32)^{1/2}$ is reasonable. Thus

$$\text{number (SSDA)} = 4(1 + 10(M/32)^{1/2}) \cdot (L - M + 1)^2 \text{ equivalent integer adds.} \quad (18)$$

Table II lists corresponding calculational costs for the several methods for various values of M and L. Values which are power of two are selected so that best figures for the FFT method might be achieved. One should note, however, that no other algorithm requires L and M to be a power of two. (It is recognized that this condition might be relaxed somewhat for the FFT, but most all available routines maintain this requirement.)

Table II shows that the given example of an SSDA is about a factor of 50 faster than the FFT correlation method. (This is a quite conservative estimate.) The order of magnitude saving by use of SSDAs is very important to production digital image processing.

V. Generalization and Conclusion

A. The General Concept of SSDA

A structure for the class of SSDAs may now be stated in a general form so that the versatility of the method is clear. There are many implementations other than those of the examples, each of which contains the following basic elements.

1) Ordering Algorithm O_1: O_1 orders the $(L-M+1)^2$ reference points. The window is successively compared to subimages which are selected by O_1. This ordering need not be fixed in advance, and may vary in a way that depends upon events occurring during the execution. In these cases, the total number of reference points which are processed is less than $(L-M+1)^2$.

2) Ordering Algorithm O_2: O_2 orders the M^2 (or fewer) windowing pairs to be compared at each reference point. O_2 may be fixed—the same for all reference points—or it may adapt in a data-dependent fashion.

3) Distance Measure (Norm) $||x||$: $||x||$ is used as a measure of error when windowing pairs are compared.

4) Sequential Measuring Algorithm Q: Q is a mapping from a subset of the M^2 possible distance measures for a particular reference point (i, j) into an element in the inspection surface $I(i, j)$.

$I(i, j)$ is directly analogous to the correlation surface described in Section III. Q operates upon distances $||x||$ for windowing pairs in the sequential manner specified by O_2. This sequence of operations continues until an event (like the passing of a threshold) occurs. At that instant $I(i, j)$ is evaluated on the basis of the measurements taken.

Each of the four basic properties may be tuned to fit a specific similarity detection problem so that a proper balance between accuracy and efficiency is realized. There are many variations that are far different from the examples presented. In the next few paragraphs, reasonable extensions to the monotonic-increasing threshold algorithm are given to show just how the general formulation can be used.

The reference points, in the examples above, were exhaustively searched. The following list presents some alternative approaches for O_1, if it is desired to sacrifice some accuracy for computation speed.

1) Apply a two-step coarse–fine uniform search, i.e., a first search on a coarse grid at every mth point and then do a full search in local regions about the maxima. (This procedure was implemented on several data sets, and a tradeoff, in fact, does exist. The degradation in accuracy is highly dependent upon the smoothness of the fully sampled $I(i, j)$ surface.)

2) Apply other multistep open-loop search criteria such as a coarse random search.

3) Apply, assuming that the surface $I(i, j)$ is monotone in some sense and has a global maximum, closed-loop hill climbing or gradient techniques.

The order for the windowing pairs O_2 might be easily changed to yield rapid elimination of misregistration points. Rather than selecting a completely random sequence, one might, for example, select a pseudorandom sequence based upon prominent features of W. That is, the first points in the sequence would be as random as possible while representing the key points for registration. There is a host of methods for the legitimate selection of feature points.

Each data structure has its own problem of normalization. SSDA may adapt to any necessary condition by the selection of suitable $||x||$. Most measures and process normalizations are acceptable. However, complex measures will somewhat degrade the ratio of saving shown in Table II.

It is apparent that there is a wide area yet unexplored for determining Q. Other mappings might be tried. It is possible, for example, to set a fixed threshold and test each of the windowing points against it independently. The surface value $I(i, j)$ might then be the number of comparisons prior to the occurrence of a certain number of threshold crossings.

Perhaps of great value to the monotonic-increasing threshold algorithm would be threshold adaptation. A conservative guess to the optimal threshold sequence might be used at first. On the basis of measurements made at succeeding reference points, the threshold sequence might be adaptively lowered. This procedure could allow an efficient algorithm to develop with very little *a priori* design on the part of the user. The algorithm would also gain a certain amount of independence from data.

B. Conclusion

A general class of sequential algorithms for similarity detection has been introduced, referencing the specific problem of translational image registration. Experimental and analytic results have been presented to show orders of magnitude improvement in efficiency. Several ideas for further improvement of experimentally implemented algoriths have also been presented.

The structure of the new algorithms is ideally suited for digital similarity detections. There is a time saving of at least 50 for typical problems on a representative medium-size computer—a prediction substantiated by experiment.

TABLE II

EQUIVALENT INTEGER ADDS FOR VARIOUS ALGORITHMS FOR SEVERAL VALUES OF L AND M

		Direct Method	FFT Correlation	Algorithm A
		$4.5M^2(L-M+1)^2$	$200\ L^2 \log_2 L$	$4(1+10(M/32)^{1/2}(L-M+1)^2$
L	M			
128	32	4.4×10^7	2.25×10^7	4.2×10^5
256	32	2.57×10^8	1×10^8	2.2×10^6
512	32	1.1×10^9	4.6×10^8*	1.05×10^7
1024	32	4.5×10^9	2×10^9*	4.35×10^7
2048	32	1.85×10^{10}	8.8×10^9*	1.75×10^8
128	64	8.15×10^7	2.25×10^7	2.5×10^5
256	64	6.9×10^8	1×10^8	2.2×10^6
512	64	3.7×10^9	4.6×10^8*	1.2×10^7
1024	64	1.7×10^{10}	2×10^9*	5.5×10^7
2048	64	7.4×10^{10}	8.8×10^9*	2.4×10^8
256	128	1.15×10^9	1×10^8	1.37×10^6
512	128	1.1×10^{10}	4.6×10^8*	1.25×10^7
1024	128	5.8×10^{10}	2×10^9*	6.7×10^7
2048	128	2.5×10^{11}	8.8×10^9*	2.9×10^8
512	256	2×10^{10}	4.6×10^8*	7.5×10^6
1024	256	1.8×10^{11}	2×10^9*	7×10^7
2048	256	1×10^{12}	8.8×10^9*	3.7×10^8
1024	512	2.7×10^{11}	2×10^9*	4.1×10^7
2048	512	2.6×10^{12}	8.8×10^9*	4×10^8
2048	1024	4.5×10^{12}	8.8×10^9*	5.7×10^8

* FFT's not possible on most machines without much disk accessing.

ACKNOWLEDGMENT

The authors wish to thank H. Kobayashi, J. Mommens, D. Grossman, and P. Franaszek for their help in many fruitful discussions.

REFERENCES

[1] P. E. Anuta, "Spatial registration of multispectral and multitemporal digital imagery using fast Fourier transform techniques," *IEEE Trans. Geosci. Electron.*, vol. GE-8, pp. 353–368, Oct. 1970.

[2] J. A. Leese, C. S. Novak, and B. B. Clark, "An automated technique for obtaining cloud motion from geosynchronous satellite data using cross-correlation," *J. Appl. Meteorol.*, vol. 10, pp. 110–132, Feb. 1971.

[3] A. Papoulis, *Probability, Random Variables and Stochastic Processes.* New York: McGraw-Hill, 1965.

[4] J. W. Goodman, *Introduction to Fourier Optics.* San Francisco: McGraw-Hill, 1968.

[5] J. W. Cooley, P. A. W. Lewis, and P. D. Welch, "Application of fast Fourier transform to computation of Fourier integrals, Fourier series, and convolution integrals," *IEEE Trans. Audio Electroacoust.*, vol. AU-15, pp. 79–84, June 1967.